Crystal Vibrations and Intermolecular Interactions of CH_3X and CD_3X (X=Cl, Br, and I)

Hideo TAKEUCHI,* Jean-Luc BRIBES,** Issei HARADA, and Takehiko SHIMANOUCHI
Department of Chemistry, Faculty of Science, The University of Tokyo, Hongo, Bunkyo-ku, Tokyo 113
(Received August 11, 1976)

Normal coordinate treatments of the crystal vibrations of methyl chloride, methyl bromide, methyl iodide, and their perdeuterated analogs have been made. The values of force constants of non-bonded atom interactions have been determined so as to give the best fit to the lattice frequencies and the splitting frequencies of the intramolecular vibrations. It has been found that the dipole-dipole interactions are essential to account for the splittings of some internal modes, but their effects on lattice frequencies are negligible.

Methyl halides are fundamental polar molecules, for which the vibrational spectra in the crystalline state have been investigated extensively. Dows[1] observed the infrared spectra of methyl chloride, methyl bromide, and methyl iodide. He[2] discussed the splittings of intramolecular vibrations of methyl chloride on the basis of the crystal structure[3] and the dipole-dipole and atom-atom interactions. Hexter,[4] Jacox and Hexter,[5] and Kopelman[6] tried to interpret the splittings of the infrared absorptions of methyl halides by considering only the dipole-dipole interaction. Harada[7] also treated the splittings and lattice vibrations of methyl chloride. However, the crystal vibrations of methyl halides have not been fully explored yet, because there has been the lack of the data on the crystal structures of CH_3Br and CH_3I and on most of the lattice vibrations.

Recently, the crystal structures of CH_3Br and CH_3I have been determined.[8] The present authors have measured the Raman spectra of crystalline CH_3X and CD_3X (X=Cl, Br, and I) and interpreted the data on the basis of the crystal structures.[9] It is now possible to investigate the intermolecular interactions in the crystals of methyl halides in detail.

In this paper, we report the results of normal coordinate analysis of the optically active crystal vibrations of methyl halides, and discuss the intermolecular interactions. The observed far-infrared spectra of the crystals are also presented, which adds to the results of an earlier study by Lafferty and Robinson.[10]

Experimental

The far-infrared spectra were measured down to 60 cm^{-1} at liquid nitrogen temperature with a Hitachi FIS-1 far-infrared spectrometer after a similar procedure as described previously.[11] The samples were of the same origins as those used for the measurements of the Raman spectra.[9] The spectra are shown in Fig. 1.

Summary of the Experimental Results

Lattice Vibrations. Assignment to a translational or a rotational lattice mode is made on the basis of the frequency shift on deuteration: The frequency shifts

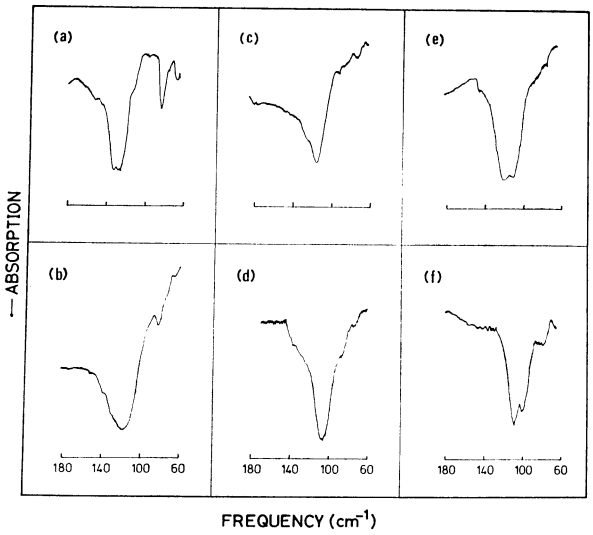

Fig. 1. Far-infrared spectra of methyl halides. (a) CH_3Cl, (b) CD_3Cl, (c) CH_3Br, (d) CD_3Br, (e) CH_3I, (f) CD_3I.

are expected to be about 30% for the rotational modes around the molecular symmetry axis and about 10% for those around the axes perpendicular to it, respectively, whereas the translational modes are expected to show no appreciable shift. Observed lattice frequencies and the assignments are summarized in Table 1.

For methyl chlorides, all the translational lattice vibrations are observed in the Raman spectra. The highest-frequency translational mode is observed also in the far-infrared spectra and therefore is assigned to either A_1 or B_2 species (see Table 2.).

Intramolecular Vibrations. Frequency splittings in the infrared spectra were observed by Dows[1] and Jacox and Hexter.[5] Frequency splittings in the Raman spectra were observed by Ito,[12] Brown and Lippincott,[13] and the present authors.[9]

The following modes are known to be perturbed by the Fermi resonance:[14] ν_1 and ν_4 of CH_3Cl, ν_1 of CH_3Br, ν_1 and ν_5 of CH_3I, and ν_1 of CD_3I.

Anomaly observed in the patterns of splitting and intensity of ν_3 mode for CH_3Cl and CD_3Cl has been ascribed to the coexistence of the chlorine isotopic (^{35}Cl and ^{37}Cl) molecules.[15]

Normal Coordinate Calculations

The calculations of the vibrational frequencies of the crystals have been performed by the use of the

* Present address: Department of Chemical Engineering and Chemical Technology, Imperial College, London SW7 2BY, England.
** Present address: Laboratoire de Spectroscopie Moléculaire, U. S. T. L. 34060, Montpellier-Cédex, France.

Table 1. Observed lattice frequencies (in cm^{-1}) of methyl halides

		CH_3Cl	CD_3Cl	CH_3Br	CD_3Br	CH_3I	CD_3I
Raman[a]							
rotational[b]	R_z	156 W	(108)				
	R_x, R_y	135 sh	124 W	119 S	106 S	113 S	100 S
		121 S	108 S	110 S	98 S	105 M	94 M
translational[c]	T_a, T_b, T_c	84 W	83 W	67 W	66 W	60 M	59 M
		71 W	68 W	60 M	60 M	49 S	48 S
		60 W	59 W	57 W	56 W		
				44 M	44 M	32 W	32 W
				39 W	38 W	28 M	27 M
Far-infrared							
rotational[b]	R_z						
	R_x, R_y	125 S, b	114 S, b	114 S, b	106 S, b	120 S	108 S
						112 S	100 S
translational[c]	T_a, T_b, T_c	82 M	82 W			55 M[d]	54 M[d]
		(41 W)[d,e]	(42 W)[d,e]	41 W[d]	41 W[d]	36 W[d]	35 W[d]

a) Ref. 9. b) R_z denotes the rotational mode about the molecular symmetry axis and R_y and R_z those about the axes perpendicular to it. c) T_a, T_b, and T_c denote the translational modes along the crystal a, b, and c axes, respectively. d) Ref. 10. e) This band may be attributed to the second-order diffraction light of 82 cm^{-1} band, since no Raman band is observed around this frequency.

Table 2. Results of factor group analysis for methyl halides

		CH_3Cl[a]	CH_3Br and CH_3I[b]
Lattice mode	translational	$A_1+A_2+B_2$	$2A_g+B_{1g}+2B_{2g}+B_{3g}+A_u+B_{1u}+B_{3u}$
	rotational	$A_1+2A_2+2B_1+B_2$	$A_g+2B_{1g}+B_{2g}+2B_{3g}+2A_u+B_{1u}+2B_{2u}+B_{3u}$
Intramolecular mode	symmetric (ν_1, ν_2, ν_3)	A_1+B_2	$A_g+B_{2g}+B_{1u}+B_{3u}$
	degenerate (ν_4, ν_5, ν_6)	$A_1+A_2+B_1+B_2$	$A_g+B_{1g}+B_{2g}+B_{3g}+A_u+B_{1u}+B_{2u}+B_{3u}$

a) Crystal structure is $Cmc2_1$ (C_{2v}^{12}), $Z=2$. A_2 mode is infrared inactive.
b) Crystal structures are isomorphous; Pnma (D_{2h}^{16}), $Z=4$. A_u mode is infrared and Raman inactive.

Table 3. Computer program CVOA for treating optically active crystal vibrations

Input
- (a) Structure data
  - (1) Unit cell dimension and atomic positions (of one molecule) in the unit-cell coordinate system, or
  - (2) Unit cell dimension and atomic positions (of one molecule) in the Cartesian coordinate system
- (b) Symmetry relationship among molecules in a unit cell
  - Matrices for rotational operations
  - Vectors for translational operations
- (c) Intramolecular coordinates and force field
  - (1) Local symmetry coordinates plus intramolecular force field, or
  - (2) Normal coordinates and normal frequencies of a free molecule
- (d) Intermolecular force field
  - (1) Functional forms of atom-atom interactions, and/or
  - (2) Force constants relating to intermolecular or inter-unit bonding (*e. g.*, hydrogen bond, bond between adjacent units in a polymer chain, *etc.*)

Output
- (a) Frequencies of intramolecular and lattice modes
- (b) Eigenvectors and Cartesian displacements
- (c) Potential energy distributions
- (d) Jacobian

GF matrix method.[16] Computer programs have been developed and the input and output of these programs are outlined in Table 3.

Positions of Atoms. The positions of heavier atoms in the crystals are taken from the data of X-ray analyses[3,8] except for that of the carbon atom of methyl iodide. The structures of methyl groups were assumed to be the same as those in the gaseous state[17] due to the lack of data on the coordinates of hydrogen atoms.

There are two possible orientations of the methyl group. We adopted the one that was preferred in the original X-ray studies[3,8] on consideration of atom-atom contacts. For methyl iodide, after a preliminary calculation the positional parameters of the carbon atom were altered from the original X-ray values (0.3144, 0.25, −0.1039) to (0.3350, 0.25, −0.1003) within the experimental errors of the X-ray analysis. This configuration gives the value (3.29 Å) of the shortest intra-layer H···I distance (in the ac plane, see Fig. 3) nearly equal to that (3.27 Å) of the shortest inter-layer one, which is consistent with the case of methyl bromide (3.02 and 3.00 Å, respectively).

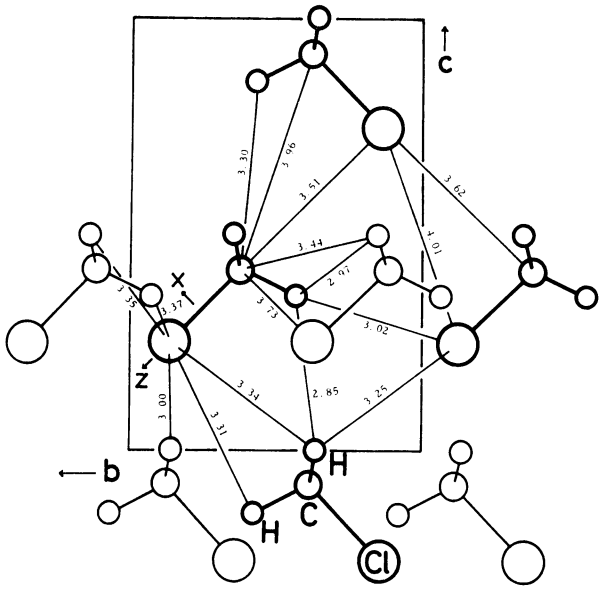

Fig. 2. Crystal structure of methyl chloride.
Interatomic distances (in Å) are indicated.

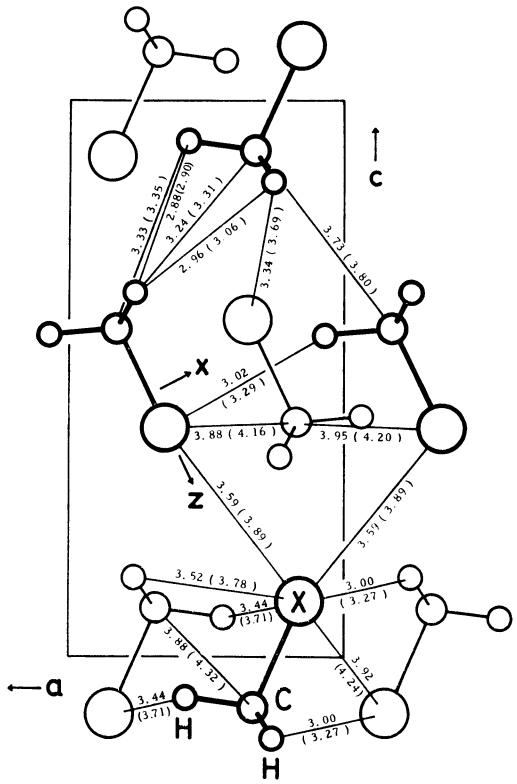

Fig. 3. Crystal structure of methyl bromide or methyl iodide.
Interatomic distances (in Å) are indicated. The values in parentheses are those for methyl iodide.

Figures 2 and 3 show the structures assumed in the calculations.

Intramolecular Potentials. The intramolecular force fields of methyl halides in the free state have been well established.[18,19] In the present calculations, the local symmetry force fields by Shimanouchi[19] are used without modification.

Intermolecular Potentials. Two sets of intermolecular potentials are assumed in the calculations. *Calculation I*: Atom-atom interaction potentials in the form,

$$V(r) = A\exp(-Br) - Cr^{-6}$$

were adopted. As for the constants A, B, and C, the

Table 4. Parameters for the atom-atom potentials

	A (mdyn Å)	B (Å^{-1})	C (mdyn Å^7)	Ref.
H···H	18.45	3.74	0.190	20
C···H	60.93	3.67	0.869	20
C···C	581.3	3.60	3.95	20
Cl···H	171.4	3.63	1.96	
Cl···C	962.0	3.56	8.92	
Cl···Cl	1592	3.513	20.2	21
Br···H	144.1	3.50	2.07	
Br···C	809.1	3.43	9.44	
Br···Br	1126	3.250	22.6	21
I···H	176.2	3.38	3.14	
I···C	988.9	3.31	14.3	
I···I	1682	3.023	51.9	21

values given by Williams(Set IV)[20] are used for H···H, H···C, and C···C pairs and those given by Dashevsky[21] are used for halogen···halogen pairs. For a pair of hydrogen···halogen or carbon···halogen type the values of potential parameters A and C are taken as the geometric means and the parameter B as the arithmetic mean of the corresponding values for the homonuclear pairs. The values of the parameters are listed in Table 4.

All the atom pairs with a distance shorter than 6.0 Å are taken into account. The second derivatives of $V(r)$'s with respect to the interatomic distances are used as the force constants.

Calculation II: Both the atom-atom interaction potential and the dipole-dipole interaction potential are taken into account.

As for the atom-atom interaction, only the short-distance pairs that are indicated in Figs. 2 and 3 are considered and the corresponding force constants are adjusted to give the best fit to the lattice and the band splitting frequencies.

The method of calculation of the force constants due to the dipole-dipole interaction is described in Appendix. The values of dipole moment derivatives with respect to the internal symmetry coordinates are calculated from the infrared intensities in the gaseous state[22] and are not varied throughout the calculations. The radius of the dipole sum sphere is set equal to 100 Å, which is found to give sufficiently converged values for the force constants.

Results

The resuts of calculations are summarized in Tables

Table 5. Calculated and observed lattice frequencies (in cm^{-1}) of CH_3Cl and CD_3Cl

Species	CH_3Cl				CD_3Cl				Mode
	Obsd	Calcd I	Calcd II	Dip.[a]	Obsd	Calcd I	Calcd II	Dip.[a]	
A_1	121	109.2	112.0	−3.6	108	97.6	99.8	−3.3	R_y
	71	75.9	72.7	−2.6	68	74.7	71.7	−2.4	T_b
A_2	156	175.2	160.7	0.0	—	124.6	115.3	−0.2	R_z
	—	96.3	108.4	−4.3	—	85.1	95.1	−3.8	R_x
	60	62.2	61.5	0.2	59	61.2	60.8	0.2	T_a
B_1	—	185.3	190.8	0.0	—	131.5	136.0	−0.2	R_z
	121	109.5	110.2	−5.0	108	98.7	98.9	−4.4	R_x
B_2	135	124.4	145.2	0.5	124	109.9	130.4	0.2	R_y
	84	85.4	83.8	−1.2	83	83.6	82.4	−0.9	T_c

a) Contributions of dipole interactions in Calculation II (see text).

Table 6. Calculated and observed lattice frequencies (in cm^{-1}) of CH_3Br and CD_3Br

Species	CH_3Br				CD_3Br				Mode
	Obsd	Calcd I	Calcd II	Dip.[a]	Obsd	Calcd I	Calcd II	Dip.[a]	
A_g	110	114.5	108.3	−1.8	98	101.6	96.3	−1.6	R_y
	67	67.1	66.2	0.1	66	66.1	65.2	0.1	T_c
	44	46.5	49.0	−0.1	44	46.3	48.7	−0.1	T_a
B_{1g}	—	138.7	134.0	0.5	—	95.2	89.4	0.2	R_z
	119	124.0	117.1	1.5	106	115.1	112.4	1.5	R_x
	57	39.1	58.2	3.7	56	39.0	56.7	2.9	T_b
B_{2g}	110	120.8	112.2	−1.4	98	107.5	99.9	−1.3	R_y
	60	65.1	64.6	−1.6	60	64.8	64.5	−1.5	T_a
	39	32.4	40.8	0.4	38	31.8	40.0	0.4	T_c
B_{3g}	—	137.6	130.8	0.6	—	94.7	88.4	0.2	R_z
	119	126.9	118.2	1.3	106	116.8	111.5	1.5	R_x
	57	40.5	58.9	3.1	56	39.2	57.7	3.6	T_b
A_u		147.5	130.6	−1.1		102.2	87.7	−0.5	R_z
		125.1	114.0	−3.7		114.8	107.8	−3.8	R_x
		25.1	31.7	3.4		24.7	31.2	3.3	T_b
B_{1u}	114	123.3	115.3	−2.9	106	110.5	103.6	−2.5	R_y
	41	49.7	43.4	−2.4	41	49.0	42.7	−2.4	T_a
B_{2u}	—	147.8	133.5	−0.5	—	102.9	89.1	−0.2	R_z
	114	123.6	115.3	−1.8	106	112.8	109.9	−1.8	R_x
B_{3u}	114	118.7	113.9	−1.8	106	106.4	102.2	−1.6	R_y
	—	67.3	64.5	−1.3	—	66.4	63.5	−1.3	T_c

a) Contributions of dipole interactions in Calculation II (see text).

Table 7. Calculated and observed lattice frequencies (in cm^{-1}) of CH_3I and CD_3I

Species	CH_3I				CD_3I				Mode
	Obsd	Calcd I	Calcd II	Dip.[a]	Obsd	Calcd I	Calcd II	Dip.[a]	
A_g	105	82.0	100.3	−1.3	94	73.9	89.5	−1.1	R_y
	60	55.8	58.9	−0.9	59	56.3	58.3	−0.9	T_c
	32	28.7	37.7	0.0	32	28.6	37.3	0.0	T_a
B_{1g}	—	104.1	151.6	0.0	—	79.3	107.6	0.2	R_z
	113	86.8	116.2	1.5	100	72.6	104.7	1.1	R_x
	49	28.5	48.5	2.1	48	28.0	47.7	2.1	T_b
B_{2g}	105	88.2	104.6	−1.0	94	78.7	93.4	−0.9	R_y
	49	46.9	52.1	−1.0	48	46.6	52.1	−0.9	T_a
	28	18.4	31.1	−0.3	27	18.1	30.8	−0.3	T_c
B_{3g}	—	99.7	147.2	0.0	—	70.4	104.1	0.0	R_z
	113	90.2	117.4	0.7	100	81.4	105.7	0.5	R_x
	49	29.2	49.4	1.2	48	28.8	48.8	1.1	T_b
A_u		100.9	147.2	0.0		71.8	103.9	−0.4	R_z
		94.3	117.0	−1.9		84.3	105.4	−1.3	R_x
		12.9	22.7	2.2		12.9	22.5	2.1	T_b
B_{1u}	112	91.4	107.5	−1.6	100	80.6	96.6	−1.4	R_y
	36	39.0	36.9	−1.4	35	38.6	36.5	−1.4	T_a
B_{2u}		105.3	151.6	0.0		80.1	107.4	−0.1	R_z
	120	90.6	115.4	−1.5	108	75.8	103.6	−1.3	R_x
B_{3u}	112	87.8	104.9	−1.4	100	78.8	94.3	−1.3	R_y
	55	54.6	55.7	−1.4	54	54.2	55.2	−1.4	T_c

a) Contributions of dipole interactions in Calculation II (see text).

Table 8. Calculated and observed splittings (in cm^{-1}) of CH_3Cl and CD_3Cl[a]

Mode	CH_3Cl					CD_3Cl				
	Obsd		Calcd I	Calcd II		Obsd		Calcd I	Calcd II	
	Infrared[b]	Raman	$\Delta\nu$	$\Delta\nu$	Dip.[c]	Infrared[b]	Raman	$\Delta\nu$	$\Delta\nu$	Dip.[c]
ν_1	—	—	0.6(A_1)	0.1(B_2)	0.5	—	—	0.3(A_1)	0.3(B_2)	0.4
			0.0(B_2)	0.0(A_1)	−0.9			0.0(B_2)	0.0(A_1)	−0.8
ν_2	10.4	—	3.3(B_2)	10.7(B_2)	0.3	7	6.3	1.5(B_2)	6.6(B_2)	0.4
			0.0(A_1)	0.0(A_1)	−0.6			0.0(A_1)	0.0(A_1)	−1.2
ν_3[d]		17.3	0.1(B_2)	6.7(B_2)	1.9		13.6	0.4(B_2)	6.5(B_2)	1.5
	8.9	9.5	0.0(A_1)	0.0(A_1)	−3.5		10.2	0.0(A_1)	0.0(A_1)	−2.7
	4.6	4.6				5.5	5.3			
ν_4	4.9	4.3	0.3(B_2)	1.8(B_2)	0.1		3.5	0.2(B_2)	1.3(B_2)	0.1
			0.2(B_1)	0.4(A_1)	−0.3			0.1(B_1)	0.3(A_1)	−0.2
			0.1(A_2)	0.0(A_2)	−0.3			0.1(A_2)	0.0(A_2)	−0.3
			0.0(A_1)	0.0(B_1)	−0.4			0.0(A_1)	0.0(B_1)	−0.3
ν_5	7.6		2.3(A_1)	7.6(A_1)	−0.6	3.2	5.0	1.4(A_1)	4.8(A_1)	−0.5
		5.9	1.1(A_2)	2.1(B_2)	0.3			0.5(A_2)	1.8(B_2)	0.3
	4.2	4.0	0.7(B_1)	1.1(A_2)	−0.6			0.1(B_1)	1.2(A_2)	−0.5
			0.0(B_2)	0.0(B_1)	−0.6			0.0(B_2)	0.0(B_1)	−0.5
ν_6	—	—	3.1(A_1)	7.3(A_1)	−0.2	—	—	2.7(A_1)	6.9(A_1)	−0.1
			1.6(A_2)	3.2(A_2)	−0.3			1.7(A_2)	0.8(A_2)	−0.1
			1.1(B_1)	1.2(B_1)	−0.3			1.0(B_1)	0.7(B_1)	−0.2
			0.0(B_2)	0.0(B_2)	0.1			0.0(B_2)	0.0(B_2)	0.0

a) Splittings are referred to the lowest-frequency component of each band. ν_1 and ν_4 of CH_3Cl are in Fermi resonance with $2\nu_5$ and $3\nu_6$, respectively. b) Ref. 1. c) Contributions of dipole interactions. d) The anomalous splittings of ν_3 are due to the chlorine isotopic compounds. See text and Ref. 15 for details.

Table 9. Calculated and observed splittings (in cm^{-1}) of CH_3Br and CD_3Br[a]

Mode		CH_3Br				CD_3Br			
			Calcd I	Calcd II			Calcd I	Calcd II	
		Obsd[b]	$\Delta\nu$	$\Delta\nu$	Dip.[c]	Obsd[b]	$\Delta\nu$	$\Delta\nu$	Dip.[c]
ν_1	IR	—	0.1	1.8	1.8	—	0.1	1.5	1.5
	R	—	0.1	0.3	0.3	—	0.2	0.2	0.2
ν_2	IR	3.1	3.2	4.3	2.8	1.9	1.4	4.3	3.7
	R	2.4	3.3	2.0	0.4	1.3	1.4	1.2	0.6
ν_3	IR	6	3.1	6.5	4.5	5.1	3.5	5.2	3.0
	R	2.5	4.2	3.6	0.7	1.7	4.5	3.6	0.5
ν_4	IR	—	0.5	0.1	0.1	—	0.3	0.3	0.1
	R	2.2	0.7	0.1	−0.3	0.8	0.5	0.1	−0.2
ν_5	IR	14.5	2.4	2.1	−0.2	11.9	1.2	1.0	−0.2
	R	5.2	3.7	3.7	0.7	5.1	2.2	2.2	0.5
ν_6	IR	5.0	6.1	5.8	−0.2	5.7	4.2	4.4	−0.1
	R	7.3	6.8	7.1	0.8	7.3	5.7	4.9	0.5

a) Absolute values are given for ν_1, ν_2, and ν_3. For ν_4, ν_5, and ν_6 maximum values are listed. The ν_1 mode of CH_3Br is in Fermi resonance with $2\nu_5$. b) The infrared data are taken from Ref. 1. c) Contributions of dipole interactions.

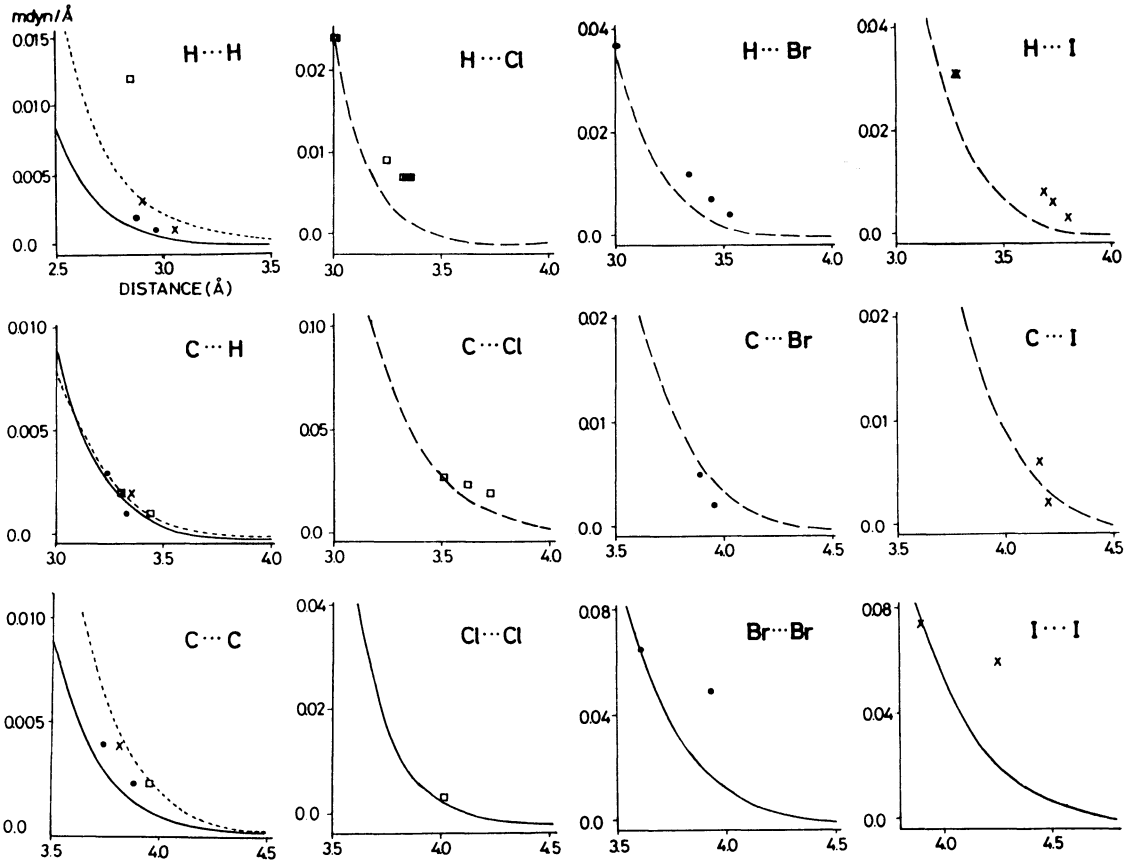

Fig. 4. Interatomic forces.
□: Methyl chloride, ●: methyl bromide, ×: methyl iodide, ——: second derivative curves of the Dashevsky potentials, ·····: second derivative curves of the Williams (Set IV) potentials, ——: second derivative curves of the hybrid potentials (see text).

TABLE 10. CALCULATED AND OBSERVED SPLITTINGS (IN cm^{-1}) OF CH_3I AND CD_3I[a]

Mode		CH_3I				CD_3I			
			Calcd I	Calcd II			Calcd I	Calcd II	
		Obsd[b]	$\Delta\nu$	$\Delta\nu$	Dip.[c]	Obsd[d]	$\Delta\nu$	$\Delta\nu$	Dip.[c]
ν_1	IR	—	0.2	1.1	1.0	—	0.1	0.7	0.7
	R	—	0.1	0.3	0.2	—	0.2	0.1	0.1
ν_2	IR	4.8	3.5	6.4	3.5	2.5	1.5	4.2	3.0
	R	2.2	3.4	3.5	0.6	1.9	1.6	1.8	0.5
ν_3	IR	4	3.5	3.7	0.6	—	3.7	3.7	0.4
	R	3.1	3.7	3.8	0.1	2.2	3.9	4.0	0.1
ν_4	IR	—	0.3	0.3	0.0	—	0.1	0.2	0.0
	R	2.8	0.1	0.4	0.1	1.3	0.1	0.3	0.1
ν_5	IR	5.9	2.2	0.5	−0.1	10.0	0.4	1.5	0.8
	R	4.7	1.9	3.0	0.3	7.1	0.1	1.8	0.5
ν_6	IR	7	3.6	3.4	0.0	7.5	3.1	3.0	0.0
	R	11.0	2.4	3.9	1.3	9.3	3.2	3.1	0.1

a) Absolute values are given for ν_1, ν_2, and ν_3. For ν_4, ν_5, and ν_6 maximum values are listed. The ν_1 and ν_5 modes of CH_3I and the ν_1 mode of CD_3I are in Fermi resonance with $2\nu_5$, $\nu_3+\nu_6$, and $2\nu_5$, respectively. b) The infrared data are taken from Ref. 1. c) Contributions of dipole interactions. d) The infrared data are taken from Ref. 5.

5—10. The values of force constants obtained in Calculation II are listed in Table 11. They are compared with the second-derivative curves of the Dashevsky and the Williams potentials in Fig. 4. Observed and calculated splittings for ν_2 and ν_3 of CH_3Br and CH_3I are compared in Fig. 5.

It is seen from the Tables 5—10 that Calculation I gives values in poor agreement with the observed except for the lattice frequencies of CH_3Cl and CD_3Cl. Especially, Calculation I fails to explain the difference in the Raman and infrared frequency splittings of ν_2 and ν_3 of CH_3Br and CH_3I. On the other hand, the lattice frequencies and frequency splittings of symmetric vibrations in Calculation II agree well with the observed except for ν_3 of methyl chlorides. The observed splittings of most of the degenerate vibrations can not be explained by either calculation. This point will be discussed in a later section.

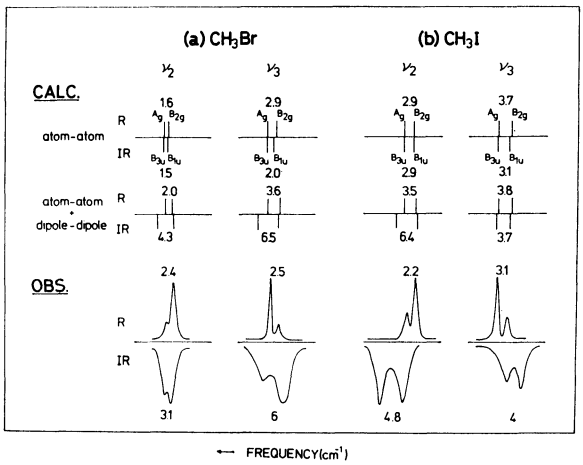

Fig. 5. Comparison of the observed and calculated splittings of ν_2 and ν_3.
(a) CH_3Br, (b)CH_3I. The values in parentheses are the splittings in cm^{-1}.

Some of the results of Calculation II are described below.

Methyl Chlorides. The vibration around 84 cm^{-1} observed in the Raman and far-infrared spectra is assigned to the translational mode along the crystal c axis (T_c) in B_2 symmetry species.

The maximum contribution of the dipole-dipole interaction to the lattice frequencies is evaluated as 5 cm^{-1}.

The splitting of ν_2 and maximum splitting of ν_5 are mainly due to the force between the hydrogen atoms at the shortest distance (2.85 Å, see Fig. 2). Therefore, the value of this force constant can be determined by fitting the calculated to the observed splittings of ν_2 and ν_5. The value thus obtained is 0.012 mdyn/Å, which corresponds to that for a distance of 2.60 Å in the Williams potential.

Although the calculated maximum splitting of ν_6 is about 7 cm^{-1}, only one band appears in each of the infrared and Raman spectra. It may be possible that the factor group components are not resolved because of their comparatively large halfwidths.

The observed splitting pattern of ν_3 is complicated by the coexistence of the chlorine isotopic molecules and simple one-to-one correspondence between the observed and calculated frequencies must be avoided. A quantitative analysis of the ν_3 splitting based on a theory of mixed crystals has shown that the calculated factor group splitting, 6.7 cm^{-1} arising mainly from the dipole-dipole interaction, accounts for the observed splitting in the Raman spectrum.[15]

The dipole-dipole interaction affects the splittings of the other modes only slightly as Dows[2] has already pointed out.

Methyl Bromides and Methyl Iodides. Calculations indicate that the frequencies of T_a mode in B_{1u} species of these molecules are mainly due to the intra-layer Br···Br or I···I interaction force. Accordingly, the values of the force constants for the intra-layer Br···

Table 11. Interatomic force constants

Molecule	Atom pair	Distance (Å)	Force constant (mdyn/Å)
Methyl chloride	H···H	2.85	0.012
		2.97	0.0
	C···H	3.30	0.002
		3.44	0.001
	C···C	3.96	0.002
	Cl···H	3.00, 3.02	0.024
		3.25	0.009
		3.31, 3.34, 3.35, 3.37	0.007
	Cl···C	3.51	0.027
		3.62	0.023
	Cl···Cl	4.01	0.003
Methyl bromide	H···H	2.88	0.002
		2.96	0.001
	C···H	3.24	0.003
		3.33	0.001
		3.40	0.0
	C···C	3.73	0.004
		3.88	0.002
	Br···H	3.00, 3.02	0.037
		3.34	0.012
		3.44	0.007
		3.52	0.004
	Br···C	3.88	0.005
		3.94	0.002
	Br···Br	3.59	0.061
		3.92	0.049
Methyl iodide	H···H	2.90	0.003
		3.06	0.001
	C···H	3.31, 3.35	0.002
	C···C	3.80	0.004
		4.32	0.0
	I···H	3.27, 3.29	0.031
		3.69, 3.71	0.009
		3.78	0.008
	I···C	4.16	0.006
		4.20	0.002
	I···I	3.89	0.073
		4.24	0.059

Br and I···I pairs with the distances of 3.59 and 3.89 Å, respectively, are determined definitely to be 0.061 and 0.073 mdyn/Å. These values agree with those expected from the Dashevsky potential. The contributions of the inter-layer Br···Br(3.92 Å) or I···I(4.24 Å) interaction force to the calculated frequencies of T_b modes in B_{1g} and B_{3g} species are about 60% and the interaction force constant is determined to be 0.049 or 0.059 mdyn/Å, respectively. These values correspond to those for distances of 3.68 and 3.97 Å in the Dashevsky potential. The calculated frequencies of the rotational vibrations, R_x and R_y, are dominated by H···H and H···X interaction forces.

The frequency splittings of ν_2 and ν_3 modes in the infrared spectra of these molecules are greater than those in the Raman spectra. The calculated frequency splittings for ν_2 and ν_3 of CH_3Br and CH_3I are in good agreement with the observed (see Fig. 5). This is because Calculation II includes the dipole-dipole interactions and the contributions from the interactions to the infrared splittings are much greater than those to the Raman splittings.

Discussion

The lack of the knowledge on the exact positions of hydrogen atoms and of the vibrational data on single crystals prevents us from discussing the results of calculation in detail. However, it may be of use to clarify the significance of factors which are assumed or disregarded in the present calculations.

First Derivative Terms. In the case of methyl chlorides, Calculation I reproduces the observed lattice frequencies well and we have examined the effects of the first derivative terms $\partial V(r)/\partial r$ of the potentials on the crystal vibration frequencies. It has been found that these terms affect the splittings negligibly as in the case of benzene,[23] while all of the lattice fre-

quencies decrease on inclusion of the terms (8% at maximum). Since the atom-atom interaction force constant is assumed independently for each atom pair in Calculation II, the corresponding linear term may also be included as an independent parameter. The linear terms may be used to lower the lattice frequencies keeping the splittings constant. Evaluation of these terms, however, is only meaningful in the case where the crystal structure and vibrational assingment are solidly established.

Splitting of the Degenerate Modes. As is described above, the agreement between the observed and the calculated splittings of degenerate vibrations in methyl bromide and methyl iodide is poor in either calculation, while the lattice frequencies and splittings of symmetric vibrations are explained by Calculation II. The situation can not be improved by simple modification of the interaction forces. One possible explanation of the large splittings of the degenerate vibrations is that the geometry and the potential of the methyl group are distorted considerably in the crystalline state. In such case, the site group splitting is expected to be far greater than the factor group splitting. In the Raman spectrum of a mixed crystal of CD_3I and CH_3I in the ratio of one to five, ν_4 and ν_5 bands of CD_3I are observed to split into doublets with the separations of 1.5 and 5.0 cm^{-1}, respectively (Fig. 6). These are assigned to the site group splittings, since no splitting is observed at this concentration for ν_3 band for which only the factor group splitting is expected to occur. Hence, it is seen that the site group splitting of ν_5 is mainly responsible for the observed splitting in pure CD_3I and that the splitting of ν_4 observed in pure CD_3I is the site group splitting. On the other hand, the calculated site-group and factor-group splittings are of the same order (2 cm^{-1} each in the case of ν_5). According to a calculation, a change of 1° in the ∠DCD angle causes 1—4 cm^{-1} splittings between $\nu_{\text{in-plane}}$ and $\nu_{\text{out-of-plane}}$ of degenerate vibrations. A slight distortion of the intramolecular potential will give similar effects. It is probable that the cooperative effects of these distortions are observed in the large splittings of the degenerate vibrations. However, these distortions of methyl group give negligible effects to the factor group splittings and lattice frequencies since the accompanying changes in the directions and distances of the atom-atom pairs are not significant.

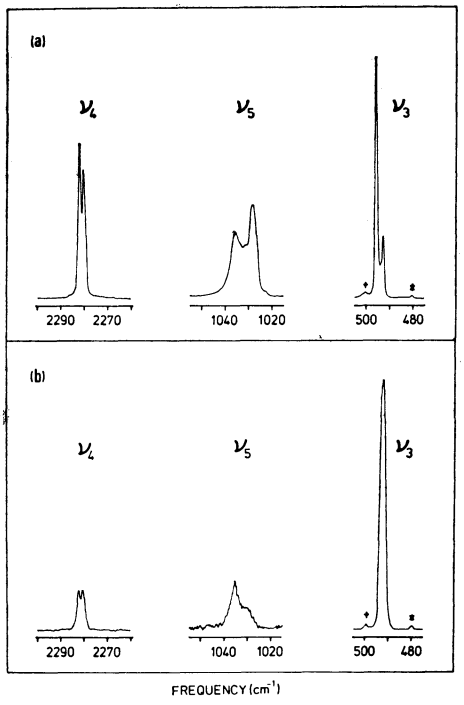

Fig. 6. Parts of the Raman spectra of methyl iodides. (a) CH_3I, (b) mixed crystal of CD_3I and CH_3I in the ratio of one to five. †: ν_3 of $^{12}CHD_2I$, *: ν_3 of $^{13}CD_3I$.

Temperature. The lattice frequencies and frequency splittings have been observed at liquid nitrogen temperature, so that we may observe the lattice vibrational bands and the band splittings as many as possible. On the other hand, the X-ray diffraction measurements have to be made at higher temperatures to avoid cracking of the crystals. The difference in temperature between two observations must also be taken into account. For this reason, Calculation I can not be simply ruled out. However, the difference in the frequency splittings of ν_2 and ν_3 in the infrared and Raman spectra in methyl bromide and methyl iodide may only be explained by taking into account the dipole-dipole interactions.

Appendix

The electrostatic interaction energy between a reference dipole and all the dipoles belonging to a sublattice β of the crystal is expressed in the tensor form

$$V = \boldsymbol{\mu}_\alpha \cdot [\sum_l (\boldsymbol{I}/r_{l\beta}^3 - 3\boldsymbol{r}_{l\beta}\boldsymbol{r}_{l\beta}/r_{l\beta}^5)\exp(-\boldsymbol{k}\cdot\boldsymbol{r}_{l\beta})] \cdot \boldsymbol{\mu}_\beta \quad \text{(A-1)}$$

where $\boldsymbol{r}_{l\beta}$ is the position vector from the reference dipole $\boldsymbol{\mu}_\alpha$ to the dipole $\boldsymbol{\mu}_{l\beta}(=\boldsymbol{\mu}_\beta)$ at the βth site in the lth unit cell and $r_{l\beta}=|\boldsymbol{r}_{l\beta}|$. $\boldsymbol{I}$ represents the identity tensor. The exponential term is the phase factor for a vibrational mode with a wave vector $\boldsymbol{k}$. The summation in the bracket of the above equation is conditionally convergent because of the long-range nature of the dipole-dipole interaction. For a slub-shaped crystal some convergent summation procedures have been developed.[24-28] For crystals of arbitrary shapes, the following approximation after the treatment of static dipole sums by Lorentz[20] will serve to avoid the troublesome convergence problem.

The sum in Eq. A-1 (hereafter signified by $\boldsymbol{T}_{\alpha\beta}$) is divided into three parts:

$$\boldsymbol{T}_{\alpha\beta} = \sum_{r_{l\beta}<R} (\boldsymbol{I}/r_{l\beta}^3 - 3\boldsymbol{r}_{l\beta}\boldsymbol{r}_{l\beta}/r_{l\beta}^5)\exp(-\boldsymbol{k}\cdot\boldsymbol{r}_{l\beta}) + \boldsymbol{T}_L + \boldsymbol{T}_S \quad \text{(A-2)}$$

The first term of this equation expresses the contribution of the dipoles inside the Lorentz sphere of radius R. $\boldsymbol{T}_L$ and $\boldsymbol{T}_S$ arise from the polarization charges on the surface of the Lorentz sphere and on the exterior surface of the crystal, respectively. The latter two influence the frequencies of infrared-active modes.

When $\boldsymbol{k}\approx 0$ (optically active modes), $\boldsymbol{T}_L$ represents the Lorentz field, $\boldsymbol{T}_L = -4\pi\boldsymbol{I}/(3V_c)$ (where V_c is the unit cell volume), and therefore Eq. A-2 leads to

$$\boldsymbol{T}_{\alpha\beta} = \sum_{r_{l\beta}<R} (\boldsymbol{I}/r_{l\beta}^3 - 3\boldsymbol{r}_{l\beta}\boldsymbol{r}_{l\beta}/r_{l\beta}^5) - 4\pi\boldsymbol{I}/(3V_c) + \boldsymbol{T}_S$$
$$= \boldsymbol{D}_{\alpha\beta} + \boldsymbol{T}_S \qquad \text{(A-3)}$$

This equation defines $\boldsymbol{D}_{\alpha\beta}$ that depends on the crystal structure but not on the shape of the crystal. On the contrary, $\boldsymbol{T}_S$ depends on the shape only.

In the spectrum of polycrystalline sample, $\boldsymbol{T}_S$ affects the band widths, since its contribution depends on the shape and orientation of each crystallite. The widths of most bands of such molecular crystals as are treated in this paper are narrow enough to show up separate band structures even in the polycrystalline state. Consequently, we may neglect the shape-dependent term $\boldsymbol{T}_S$. In this approximation, Eq. A-1 reduces to

$$V = \boldsymbol{\mu}_\alpha \boldsymbol{D}_{\alpha\beta}\boldsymbol{\mu}_\beta \qquad \text{(A-4)}$$

This expression is equivalent to that for the transverse mode in the infinite crystal.[30]

The dipole moment of a unit molecule in the crystal is expanded in powers of displacement coordinates $\boldsymbol{S}$:

$$\boldsymbol{\mu} = \boldsymbol{\mu}^\circ + \sum_i \frac{\partial \boldsymbol{\mu}}{\partial S_i} S_i + \frac{1}{2}\sum_{i,j} \frac{\partial^2 \boldsymbol{\mu}}{\partial S_i \partial S_j} S_i S_j + \cdots \qquad \text{(A-5)}$$

where $\boldsymbol{\mu}^\circ$ is the permanent dipole moment. It may be reasonable to assume that the dipole is located at the center of gravity of the molecule. Substituting Eq. A-5 into Eq. A-4, we obtain the optically-active potential energy matrix element $f_{\alpha\beta}^{ij}$ due to the dipole-dipole interaction:

$$f_{\alpha\beta}^{ij} = \frac{\partial \boldsymbol{\mu}_\alpha}{\partial S_i} \cdot \boldsymbol{D}_{\alpha\beta} \cdot \frac{\partial \boldsymbol{\mu}_\beta}{\partial S_j} \qquad \text{(A-6)}$$

$$f_{\alpha\alpha}^{ij} = \frac{\partial^2 \boldsymbol{\mu}_\alpha}{\partial S_i \partial S_j} \boldsymbol{D}_{\alpha\alpha}\boldsymbol{\mu}_\alpha \qquad \text{(A-7)}$$

The intermode coupling terms $f_{\alpha\beta}^{ij}(i \neq j)$ may be neglected in first order approximation.

For intramolecular modes the value of $\partial\boldsymbol{\mu}/\partial S_i$ is calculated from the infrared absorption intensity in the gaseous state (the oriented gas model), whereas $\partial^2\boldsymbol{\mu}/\partial S_i^2$ is not available at the present stage. The force constant $f_{\alpha\alpha}^{ii}$ arising from $\partial^2\boldsymbol{\mu}/\partial S_i^2$ contributes to the band shift alone. Therefore we can neglect it in treating only the splittings of internal modes.

For a rotational lattice mode, both of $\partial\boldsymbol{\mu}/\partial S_i$ and $\partial^2\boldsymbol{\mu}/\partial S_i^2$ are evaluated analytically by differentiating the permanent dipole with respect to the rotational coordinate. The forces associated with translational motions can be obtained from Eq. A-4 by numerical differentiation.

References

1) D. A. Dows, *J. Chem. Phys.*, **29**, 484 (1958); *ibid.*, **33**, 1743 (1960).
2) D. A. Dows, *J. Chem. Phys.*, **32**, 1342 (1960); *ibid.*, **35**, 282 (1962).
3) R. D. Burbank, *J. Am. Chem. Soc.*, **75**, 1211 (1953).
4) R. M. Hexter, *J. Chem. Phys.*, **33**, 1833 (1960).
5) M. E. Jacox and R. M. Hexter, *J. Chem. Phys.*, **35**, 183 (1961).
6) R. Kopelman, *J. Chem. Phys.*, **44**, 3547 (1966).
7) I. Harada, Ph. D. Thesis, The University of Tokyo, Tokyo, 1967.
8) T. Kawaguchi, M. Hijikigawa, Y. Hayafuji, M. Ikeda, R. Fukushima, and Y. Tomiie, *Bull. Chem. Soc. Jpn.*, **46**, 53 (1973).
9) H. Takeuchi, J. -L. Bribes, I. Harada, and T. Shimanouchi, *J. Raman Spectrosc.*, **4**, 235 (1976).
10) W. L. Lafferty and D. W. Robinson, *J. Chem. Phys.*, **36**, 83 (1962).
11) I. Harada and T. Shimanouchi, *J. Chem. Phys.*, **46**, 2708 (1967).
12) M. Ito, *J. Chem. Phys.*, **40**, 3128 (1964); *ibid.*, **41**, 2842 (1964).
13) C. W. Brown and E. R. Lippincott, *J. Chem. Phys.*, **52**, 786 (1970).
14) T. Shimanouchi, "Tables of Molecular Vibrational Frequencies," Consolidated Vol. 1, Nat. Stand. Ref. Data Ser., Nat. Bur. Stand. (U. S.), 39, U. S. Gov. Printing Office, Washington, D. C. (1972).
15) H. Takeuchi, I. Harada, and T. Shimanouchi, *Chem. Phys. Lett.*, **43**, 516 (1976).
16) T. Shimanouchi, M. Tsuboi, and T. Miyazawa, *J. Chem. Phys.*, **35**, 1597 (1961).
17) J. L. Duncan, *J. Mol. Struct.*, **6**, 447 (1970).
18) J. L. Duncan, A. Allan, and D. C. Mckean, *Mol. Phys.*, **18**, 289 (1970).
19) T. Shimanouchi, "Physical Chemistry," Vol. 4, H. Eyring, D. Henderson, and W. Jost, ed, Academic Press (1970), Chap. 6.
20) D. E. Williams, *J. Chem. Phys.*, **46**, 4680 (1967).
21) B. G. Dashevsky, *Zh. Strukt. Khim.*, **11**, 912 (1970).
22) A. D. Dickson, I. M. Mills, and B. Crawford, Jr., *J. Chem. Phys.*, **27**, 445 (1957).
23) G. Taddei, H. Bonadeo, M. P. Mazocchi, and S. Califano, *J. Chem. Phys.*, **58**, 966 (1973).
24) B. R. A. Nijboer and F. W. de Wette, *Physica*, **23**, 309 (1957)
25) F. W. de Wette and G. E. Schacher, *Phys. Rev.*, **137A**, 78 (1965).
26) P. P. Ewald, *Ann. Phys.*, **64**, 253 (1921).
27) H. Kornfeld, *Z. Phys.*, **22**, 27 (1924).
28) M. H. Cohen and F. Keffer, *Phys. Rev.*, **99**, 1128 (1955).
29) H. A. Lorentz, "The Theory of Electrons and Its Application to the Phenomena of Light and Radiant Heat," Dover, New York (1952).
30) J. C. Decius, *J. Chem. Phys.*, **49**, 1387 (1968).